

## A NOVEL PWM TECHNIQUE FOR INTEGRATED BOOST RESONANT CONVERTERS FOR AC APPLICATIONS

Rose Philip<sup>1</sup>, Prof A.Balamani<sup>2</sup>

P G scholar, Karpaga Vinaya College of Engineering and Technology,Chennai, India<sup>1</sup>  
Professor and Head ,Karpaga Vinaya College of Engineering and Technology,Chennai, India<sup>2</sup>  
rosephilip1989@gmail.com<sup>1</sup>, ayyabal@gmail.com<sup>2</sup>

### ABSTRACT

Effective photovoltaic power conditioning requires well-organized power conversion and accurate maximum power point tracking to neutralize the effects of panel mismatch, shading, and variation in power output during a daily cycle. This project presents a unique method for widening the input range of pulse-width modulation (PWM) of integrated resonant converters and it maintains high conversion efficiency. The technique primarily unites constant-on, constant off, and fixed-frequency control depending on the required duty cycle. With hybrid-frequency control, the circuit also retains zero current switching for the output diodes, minimizes switching loss, and eliminates circulating energy at the transformer across the entire operating range.

**Keywords** PWM, ZVS, Integrated resonant converter, MPPT, ZCS.

### I. INTRODUCTION

Rising prices for traditional fossil fuel sources, coupled with rapidly falling prices for polycrystalline silicon panels, has resulted in an increased acceptance rate for PV systems. The voltage obtained is less, so it has to be boosted up to a high value for various applications. Here Integrated Boost converter with closed loop control is focused.

With the most primitive switched-mode power converters, it became evident that higher frequencies allow smaller L's and C's and this result in smaller, lighter, and less costly systems. The down side to moving to higher frequencies, however, are the problems of greater vulnerability to parasitic capacitance and leakage inductance, larger stress in the switching devices, and increased EMI and RFI.

A typical DC-DC converter is encompasses of active switches such as MOSFETs or IGBTs, diodes, magnetic components for example inductors and transformers, and static devices like capacitors. Magnetic components are heavier and needs more volume than any other parts in a power electronic converter. The size of the magnetic components is conversely proportional to the switching frequency of the DC-DC converter. In order to decrease the volume and weight of converter, higher switching frequency must be chosen<sup>[1]</sup>.

A resonant mode system proffers the potential of obtaining the benefits while avoiding many of the disadvantages of higher frequencies. With a resonant circuit in the power path, the switches can be arranged to operate at either zero current or voltage

points in the waveform, greatly reducing their stress levels; the resonant sine wave minimizes higher frequency harmonics reducing noise levels; and since the circuit now needs inductance and capacitance, parasitic elements may improve rather than detract from circuit performance. With the benefits power systems operating in the range of 500 kHz to 2.0 MHz are practical and in fact are already being produced by a few pioneering manufacturers<sup>[2]</sup>.

#### A. Boost Converter

The boost is an acknowledged non-isolated power stage topology, sometimes called a step-up power stage. Power supply designers desires the boost power stage because the needed output is always more than the input voltage. The input current for a boost power stage is unremitting, or non-pulsating, because the output diode conducts simply during a segment of the switching cycle. The output capacitor provides the entire load current for the remaining of the switching cycle.

A power stage can work in continuous or discontinuous inductor current mode. In continuous inductor current mode, current flows continuously in the inductor during the whole switching cycle in steady-state operation<sup>[3]</sup>. In discontinuous inductor current mode, inductor current is zero for a segment of the switching cycle. It begins at zero, achieves peak value, and return to zero through each switching cycle. It is advantageous for a power stage to stay in only one mode over its expected operating conditions because

the power stage frequency response alters significantly between the two modes of operation.

### B. Integrated Boost Resonant Converters

The boost action when integrated into the resonant converter forms an integrated boost converter. Allows the resonant action to add four primary benefits:

- 1) The output diodes D1 and D2 attain zero current switching (ZCS);
- 2) Switching loss in the primary-side MOSFETs is equal to a standard synchronous boost;
- 3) The transformer has no circulating energy;
- 4) The resonant stage gain is fixed and equivalent to the transformer turns ratio (1:n) [4].

## II. OPERATION OF THE PROPOSED SYSTEM

### A. Block Diagram

The block diagram of the proposed system is shown below. The system is having a closed loop control. In other words it can be called as feedback control. Feedback control increases the accuracy and the robustness of the system.

The input to the system is small DC voltage at around 9v to 12v from solar panel. In this project the maximum power point of the solar panel is tracked using Perturb and Observation technique.

The IBR circuit contains

1. Boost circuit consisting of an inductor and four MOSFETs
2. Resonant circuit consisting of four capacitors and leakage inductor [5].

The DC input to full bridge inverter is inverted to AC and given to the primary of high frequency transformer, it is then rectified using diode full bridge and given to the load. The gate pulses to the MOSFETs are given by the controller circuit, which in turn is produced based on the difference between the reference voltage from MPPT and IBR's output voltage.

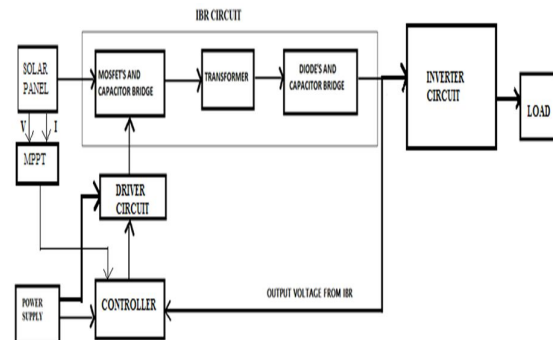


Fig. 2.1 Block Diagram of proposed System

While designing the hardware an opto-coupler will be placed in between the controller and the IBR circuit. This is done in order to isolate the high voltage power circuit from low voltage controller part.

### B. Circuit Topology

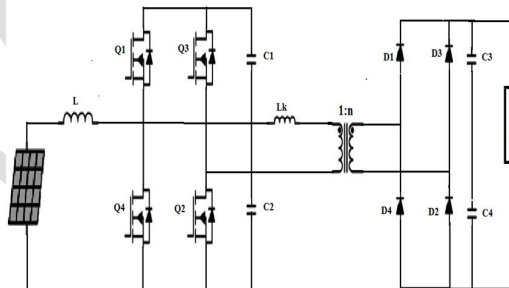


Fig. 2.2 Circuit Topology of proposed System

The circuit can operate in a wide range of duty cycle which is automatically adjusted and hence switching period can be changed continuously. Here the width of the pulses given to the switches are varying automatically based on the insolation to ensure maximum power at the output. Both fixed frequency control and variable frequency control, based on feedback is possible. Double bridge IBR circuit is proposed for further improving the voltage gain.

The circuit has a boost part, which encompasses an inductor and four switches. The resonant part includes four capacitors namely C1, C2, C3 and C4 along with the leakage inductor. Because Q1, Q2 and Q3, Q4 are switched complementary to one another, the input inductor L operates in the continuous conduction mode (CCM) and under no conditions becomes discontinuous. The inductor current rises linearly during modes 3 and 4, and decreases linearly during modes 1 and 2. The energy transfer between the combinations of C1, C2 and C3,

C4 is resonant, occurring only during modes 1 and 3. Though the boost converter is integrated into the resonant circuit, the two elements are effectively decoupled as long as the resonant modes are allowed to fully complete. Thus, the consequent voltage gain is merely the product of a boost converter voltage gain and the gain of the resonant stage.

#### Mode 1

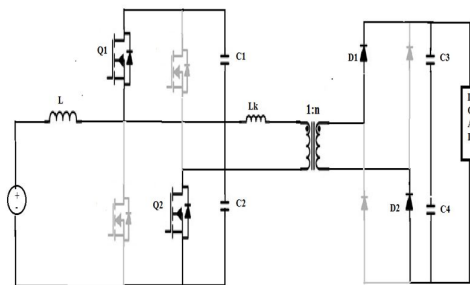


Figure 2.3 Circuit for Mode 1 Operation

Beginning with the turn off of Q3 and Q4 preceding to  $t_0$ , the current in the input inductor L flows into the body diode of Q1, discharging its parasitic capacitance and charging C1 and C2. Therefore Q1 is turned ON under ZVS conditions at  $t_0$ . The upper input-side capacitor C1 starts resonating with the transformer leakage inductance  $L_k$  and the output-side capacitors, C3 and C4, through D1 and D2. Once the transformer current resonates back to zero, D1 and D2 prevents the continue resonating in the reverse direction, ending mode 1. The length of mode 1 is given by

$$T_{res1} = \pi \sqrt{\frac{L_k}{C_1 + C_2 + n^2(C_3 + C_4)}}$$

#### Mode 2

Q1 and Q2 are still active, however it only conduct the input inductor current. The resonant elements conduct zero current during this interval. Mode 2 ends with the turn-off of Q1 and Q2 and later the turn-on of Q3 and Q4.

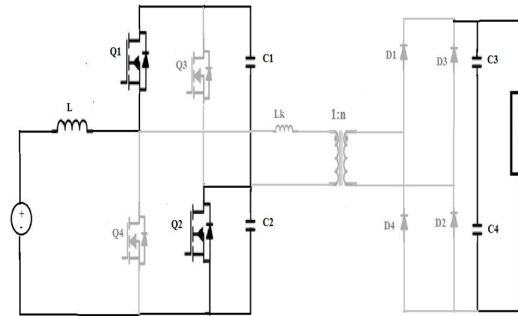


Figure 2.4 Circuit for Mode 2 Operation

#### Mode 3

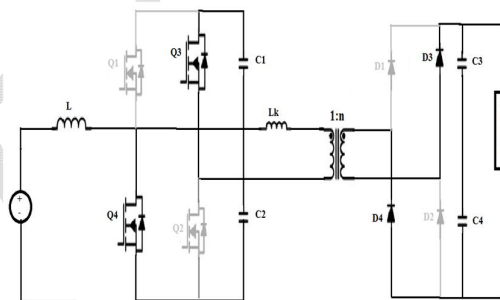
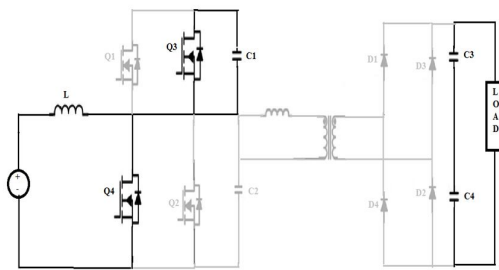


Figure 2.5 Circuit for Mode 3 Operation

After the turn-off of Q1 and Q2, but prior to the turn-on of Q3 and Q4, the inductor current is still charging the series combination of C1 and C2, through the body diode of Q1. When Q3 and Q4 are turned ON, the body diode of Q1 and Q2 are hard commutated. At  $t_2$ , C2 starts to resonate with  $L_k$  and the parallel combination of C3 and C4, through the diode D2. Simultaneously, the inductor current rises linearly through Q2. Once the transformer current resonates back to zero, D2 blocks the continued oscillation, marking the end of mode 3.

$$T_{res2} = \pi \sqrt{\frac{C_2 \times n^2 (C_3 + C_4)}{C_2 + n^2 (C_3 + C_4)}}$$

*Mode 4*



**Figure 2.6 Circuit for Mode 4 Operation**

The inductor current continues to flow through the lower device, increasing until Q3 and Q4 turned off and the circuit returns to mode 1.

### III. CLOSED LOOP CONTROL TECHNIQUE

The input voltage reference is generated by the maximum-power-point tracking (MPPT) loop, passing a reference to the input voltage control loop<sup>[6]</sup>.

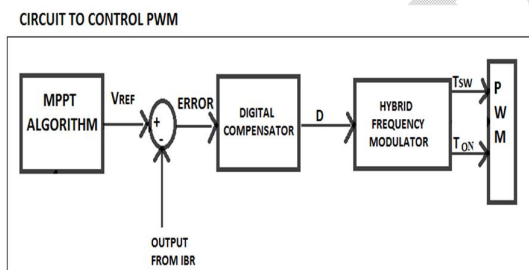


**Figure 3.1 Closed loop control technique**

The usual output of the digital compensator is the only required input to the hybrid-frequency modulator, and the output works normally with a PWM comparator that requires both a switching period length and a value for the main switch on-time<sup>[7]</sup>. Once the required on-time and the maximum switching period are determined, each individual duty ratio corresponds to one switching period and on-time combination.

### IV. SWITCHING PERIOD ANALYSIS UNDER PROPOSED MODULATION

The converter operates in constant on-time control for duty ratios less than 50%<sup>[8]</sup>. The converter

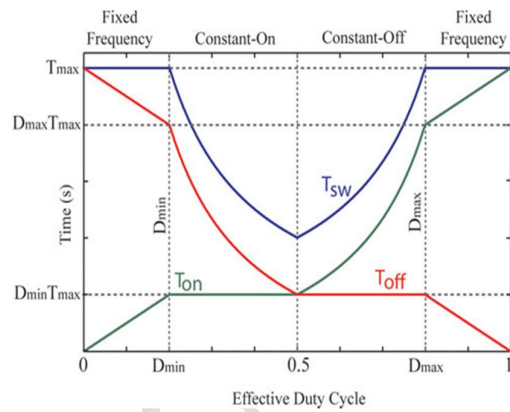


**Figure 4.1 Switching Period Analysis Under Proposed Modulation**

operates in constant off-time control for duty ratios greater than 50%. Thus along the designed operating range, neither the on-time nor the off-time will decrease below a specified minimum. The total switching period, defined as the sum of the on-time and off-time, reaches a minimum at 50% duty cycle, reducing the ac flux density in the transformer. For duty ratios outside the desired operating range, the converter operates in fixed frequency<sup>[9]</sup>.

**TABLE 1**  
*Table showing various  $T_{sw}$ ,  $T_{on}$  and  $T_{off}$*

	FIXED FREQUENCY	CONSTANT-ON	CONSTANT-OFF
$T_{sw}$	$T_{max}$	$\frac{T_{max} D_{min}}{D}$	$\frac{T_{max} D_{min}}{1-D}$
$T_{on}$	$D \cdot T_{max}$	$D_{min} T_{max}$	$T_{max} D_{min} (\frac{D}{1-D})$
$T_{off}$	$(1-D)T_{max}$	$T_{max} D_{min} (\frac{1-D}{D})$	$D_{min} T_{max}$

*Flowchart*

The hybrid frequency modulator in the simulation uses a MATLAB program which is based on the above flowchart.

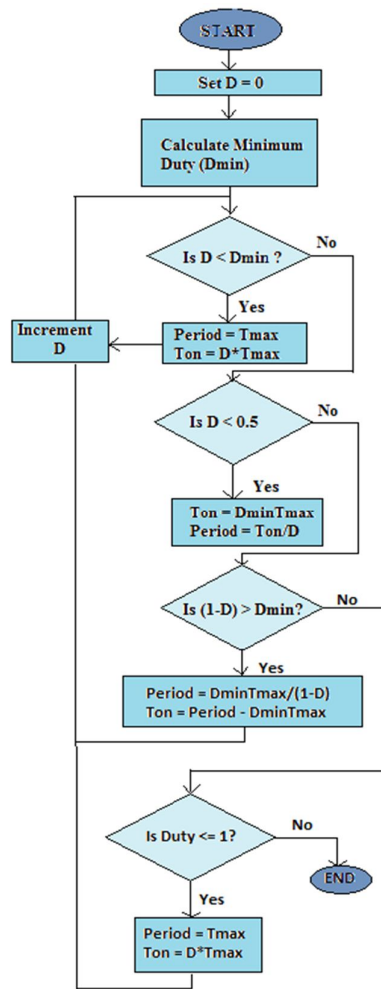


Figure 4.2 Flowchart for Frequency Modulation.

## V. SIMULATION

### A. Simulation Circuit

The figure below shows the simulation circuit of the entire project showing solar panel<sup>[10]</sup> connected as the input to the full bridge IBR circuit. The pulses to the switches are generated through MATLAB program<sup>[11]</sup>.

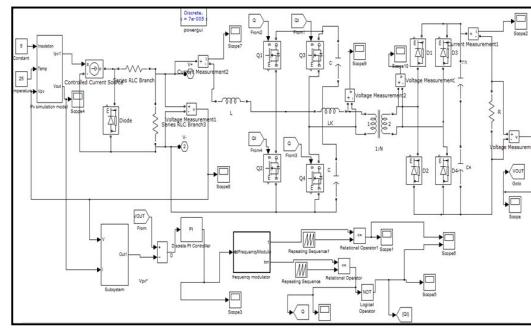


Figure 5.1 Complete Simulation Circuit

### B. Simulation Results

The various simulation results are given below. The simulation result for input voltage from the solar panel is shown in Fig 5.2. Its value is 11V and the input current from solar panel is shown in Fig.5.3. Its value is 0.43A.

The simulation result for primary side voltage of transformer is shown in Fig.5.4 with 30V. The secondary side voltage of transformer is shown in Fig.5.5 with a value of 194V. The output voltage across the IBR circuit is shown in the diagram Fig.5.6. Its value is 193V. The simulation result for output current of IBR circuit is shown in Fig.5.7, with a value of 0.0193A. The output voltage of inverter circuit is about 230V.

The pulses generated using MATLAB program for the switches Q1 and Q2 is shown in Fig.5.9.

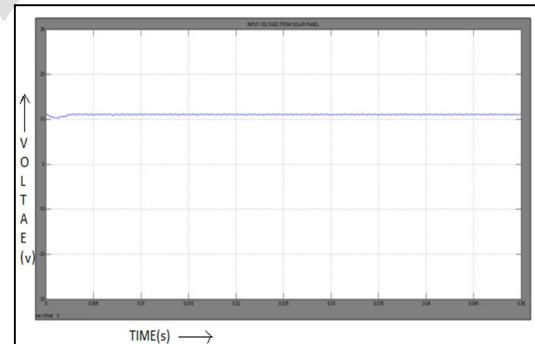


Figure 5.2 Input Voltage from Solar Panel.

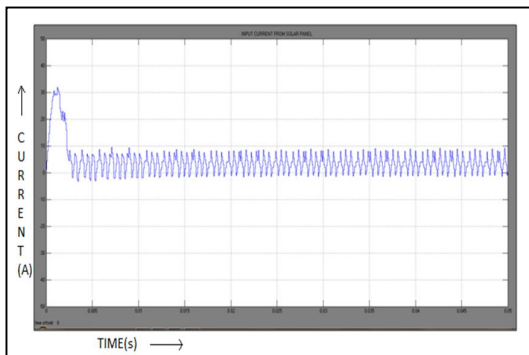


Figure.5.3 Input Current From Solar Panel.

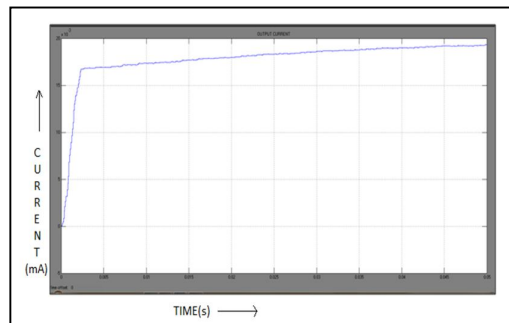


Figure.5.7 Output Current of IBR Circuit

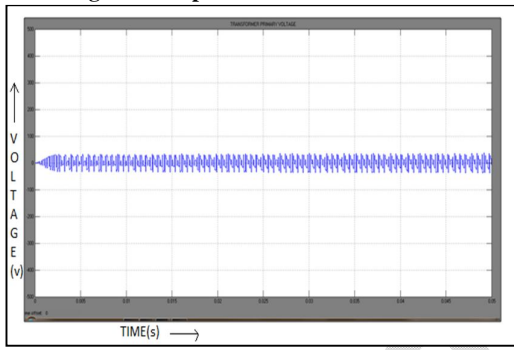


Figure.5.4 Primary Voltage of Transformer

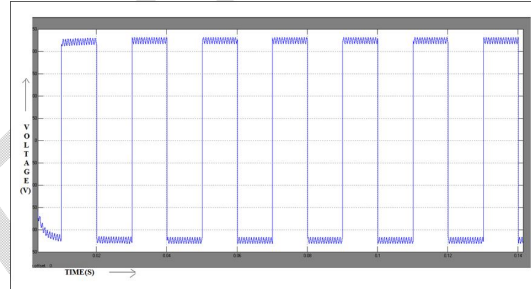


Figure.5.8 Output Voltage of Inverter Circuit

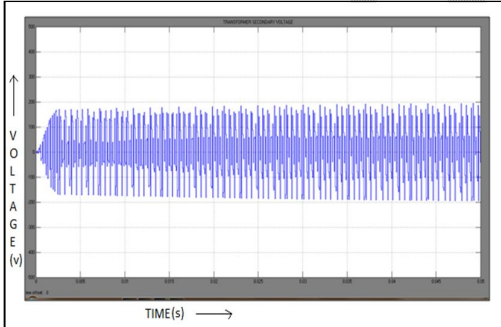


Figure.5.5 Secondary Voltage of Transformer

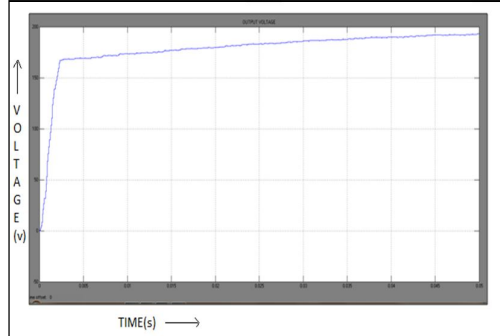
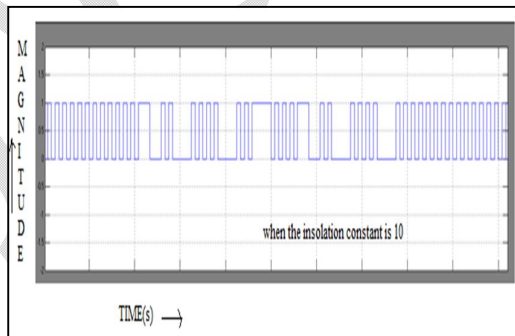


Figure.5.6 Output Voltage of IBR Circuit.

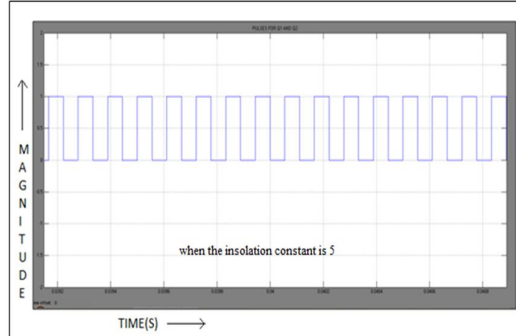


Figure 5.9 Pulses Generated for Q1 and Q2 at various insulations.

## VI. CONCLUSIONS

The small DC voltage from Solar Panel is boost up to a high value using full bridge IBR circuit. Solar panel is modeled with MPPT technique to ensure maximum power is been obtained. The algorithm uses fixed frequency, constant-on, and constant off techniques depending on the required duty cycle. Thus at high or low duty cycles, the converter operates under fixed frequency control to limit the maximum switching period and prevent magnetic saturation. The closed loop control technique developed thus provides a high voltage gain.

## REFERENCES

- [1] C.-A. Yeh and Y.-S. Lai, "Digital pulse width modulation technique for a synchronous buck dc/dc converter to reduce switching frequency," *IEEE Trans. Ind. Electron.*, vol. 59, no. 1, pp. 550–561, Jan. 2012.
- [2] R Beiranvand, B.Rashidian,M.R.Zolghadri, and S.M.H.Alavi, "Optimizing the normalized dead-time and maximum switching frequency of a wide-adjustable-range LLC resonant converter," *IEEE Trans. Power Electron.*, vol. 26, no. 2, pp. 462–472, Feb. 2011.
- [3] J.Sun, "Small-signal modeling of variable frequency pulse width modulators," *IEEE Trans. Aerosp. Electron. Syst.*, vol. 38, no. 3, pp. 1104–1108, Jul. 2002
- [4] C.-E. Kim, G.-W. Moon, and S.-K. Han, "Voltage doubler rectified boost integrated half bridge (VDRBHB) converter for digital car audio amplifiers," *IEEE Trans. Power Electron.*, vol. 22, no. 6, pp. 2321–2330, Nov.2007
- [5] Z. Liang, R. Guo, J. Li, and A. Q. Huang, "A high-efficiency PV module integrated dc/dc converter for PV energy harvest in FREEDM systems," *IEEE Trans. Power Electron.*, vol. 26, no. 3, pp. 897–909, Mar. 2011.
- [6] Simulation & Proposed Hardware Implementation of MPPT controller for a Solar PV system." International Journal of Advanced Electrical and Electronics Engineering, (IJAEEE)
- [7] An Integrated Boost Resonant Converter for Photovoltaic Applications",, *IEEE TRANSACTIONS ON POWER ELECTRONICS*, VOL. 28, NO. 3, MARCH 2013
- [8] Mathematical Modeling of Photovoltaic Module with Simulink.
- [9] M. H. Todorovic, L. Palma, and P. N. Enjeti, "Design of a wide input range dc-dc converter with a robust power control scheme suitable for fuel cell power conversion," *IEEE Trans. Ind. Electron.*, vol. 55, no. 3, pp. 1247–1255, Mar. 2008.
- [10] X.Wang, F. Tian, and I. Batarseh, "Highefficiency parallel post regulator for wide range input dc-dc converter," *IEEE Trans. Power Electron.*, vol. 23, no. 2, pp. 852–858, Mar. 2008.
- [11] [www.mathworks.com](http://www.mathworks.com)